

## Research Article

# Synthesis, cytotoxicity, apoptosis and molecular docking studies of novel phenylbutyrate derivatives as potential anticancer agents

Azar Mostoufi<sup>a,b</sup>, Raheleh Baghcoli<sup>b</sup>, Masood Fereidoonnehzad<sup>b,c,\*</sup>

<sup>a</sup> Cancer, Environmental and Petroleum Pollutants Research Center, Ahvaz Jundishapur University of Medical Sciences, Ahvaz, Iran

<sup>b</sup> Department of Medicinal Chemistry, School of Pharmacy, Ahvaz Jundishapur University of Medical Sciences, Ahvaz, Iran

<sup>c</sup> Toxicology Research Center, Ahvaz Jundishapur University of Medical Sciences, Ahvaz, Iran

## ARTICLE INFO

## Keywords:

Phenylbutyrate derivatives

Synthesis

Cytotoxic activity

Apoptosis

Docking

## ABSTRACT

Phenylbutyrate (PB), a small aromatic fatty acid, has been known as an interesting compound with the ability of anti-proliferation and cell growth inhibition in cancer cells. In the present study, a series of PB derivatives were synthesized by Passerini multicomponent reaction and their cytotoxic activities against various human cancer cell lines including A549 (non-small cell lung cancer), MDA-MB-231 (breast cancer), and SW1116 (colon cancer) were evaluated. The results revealed that **B9**, displayed significantly higher *in vitro* cytotoxicity with IC<sub>50</sub> of 6.65, 8.44 and 24.71 μM, against A549, MDA-MB-231 and, SW1116, respectively, in comparison to PB. The effects of these compounds on the proliferation of MCF-10A as non-tumoral breast cell line, showed good selectivity of the compounds between tumorigenic and non-tumorigenic cell lines. Moreover, **B9** has indicated apoptosis-inducing activities to MDA-MB-231 cancer cell line in a dose-dependent manner. The molecular docking studies of the synthesized compounds on pyruvate dehydrogenase kinase 2 (PDK2; PDB ID: 2BU8) and histone deacetylase complex (HDAC; PDB ID: 1C3R), as the main targets of PB were applied to predict the binding sites and binding orientation of the compounds to these targets.

## 1. Introduction

Compelling recent evidence suggests the growth, proliferative and survival of cancer cells are strongly associated with altered metabolism (Seyfried and Shelton, 2010). Most of the cancer cells rely on glycolysis as the primary energy source instead of mitochondrial respiration, even in the presence of excess oxygen (Rajendran et al., 2004). This phenomenon leads to high lactate release, which affects the tumors metastatic and progression. At the same time, it may cause the suppression of mitochondrial function and resistance mitochondrial-dependent apoptosis. This metabolic phenotype is well-known as the Warburg effect (Doherty and Cleveland, 2013; Warburg et al., 1927). Recent studies show Phenylbutyrate (PB) treatment is impacting on cellular metabolic pathways as an inhibitor of pyruvate dehydrogenase kinase (PDK) and thus lead to changes the cancer cell metabolic remodeling (Ferriero and Brunetti-Pierri, 2013; Ferriero et al., 2013, 2014). PB has hopeful futures in cancer treatment. Although, its basic molecular mechanisms is not understood (Jin et al., 2017).

The PDK / pyruvate dehydrogenase complex (PDHC) axis is an important regulatory step, which links glycolysis to the tricarboxylic acid (TCA) cycle through the irreversible conversion of pyruvate to

acetyl-CoA. In a variety of cancers, the high level of transcription of PDK results in the selective inhibition of PDHC (Zhang et al., 2015). PB as a novel anticancer agent can increase the activity of PDHC enzyme by inhibition of PDK and shifts the metabolism of cancer cells from the state of glycolysis to glucose oxidation (GO). By restore mitochondrial respiration and phosphorylation oxidative via “forcing” pyruvate’s entry into the mitochondria in cancer cells, dissipation of mitochondria membrane potential, activation of several proteins that play a key role in the apoptotic signaling pathway causes apoptosis associated with mitochondria and decrease the growth of cancer cells (Zhang et al., 2017).

Another mechanism that takes into account for anticancer effects of PB is various effects on gene expression as an inhibitor of histone deacetylases (HDACs), which has been used for clinical trials in various cancers (Donohoe et al., 2012; Iannitti and Palmieri, 2011). This effect prevents the deacetylation of histone and increased the availability of transcription factors to promoter regions in the DNA and accordingly control gene expression that explain the impact of PB on the expression of important regulators of apoptosis and cell cycle (Gore et al., 1997; Kusaczuk et al., 2016; Li et al., 2012).

Furthermore, PB has been previously approved by FDA for human

\* Corresponding author at: Department of Medicinal Chemistry, School of Pharmacy, Ahvaz Jundishapur University of Medical Sciences, Ahvaz, Iran.

E-mail address: [Fereidoonnehzad-m@ajums.ac.ir](mailto:Fereidoonnehzad-m@ajums.ac.ir) (M. Fereidoonnehzad).

use in the treatment of urea cycle defects (Burrage et al., 2014). Also, it is used as a candidate for treating neurological diseases such as Alzheimer's disease (AD) (Ricobaraza et al., 2009), Parkinson's disease (PD) (Gardian et al., 2004), Huntington's disease (HD) (Singh et al., 2006), Type 2 diabetes (Özcan et al., 2006) and Lactic acidosis (Ferriero et al., 2013).

Our research work was conducted to find new PB derivatives with better biological activity than PB. Here, we report the synthesis of novel PB derivatives using Passerini multicomponent reaction and their cytotoxicity against human cancer cell lines and normal cell line, as well as their apoptosis and molecular docking studies on pyruvate dehydrogenase kinase 2 (PDK2; PDB ID: 2BU8) and histone deacetylase complex (HDAC; PDB ID: 1C3R) were acquired.

## 2. Result

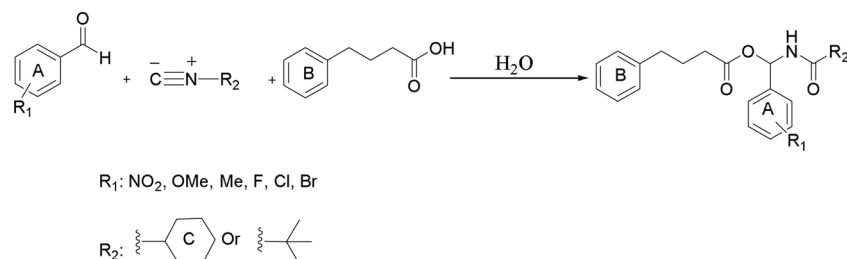
### 2.1. Chemistry

In the present study, PB analogs have been prepared through the Passerini multicomponent reaction by known literature method (Dömling, 2002) from the respective aldehyde derivatives, isocyanide and phenylbutyrate in standard condition (Scheme 1). In case of gross product creation, it was purified with recrystallization or on chromatography plate, using silica gel and solution 50% or 25% ethyl acetate in *n*-hexane. The products were characterized by their spectral (IR, <sup>1</sup>HNMR, <sup>13</sup>CNMR) and physical data (Melting point). The chemical profile of the compounds is shown in Table 1.

### 2.2. Biological evaluation

So far, among the known anti-tumor agents, PB and its derivatives are an important class of molecules with beneficial effect for cancer treatment (Jeng et al., 2006; Villar-Garea and Esteller, 2004; Rada-Iglesias et al., 2007). Here, we synthesized PB derivatives and evaluated their anticancer activity against the three human cancer cell lines including A549 (human lung adenocarcinoma epithelial cell line), MDA-MB-231 (breast cancer), and SW1116 (colon cancer). Furthermore, to show the selectivity of the compounds between normal and cancerous cell lines, the toxic effects of these compounds were also conducted on the normal breast cell line (MCF-10A). The IC<sub>50</sub> of the Compounds for each studied cancer cell line is presented in Table 2. Nearly, all the synthetic compounds had higher cytotoxicity activity than PB. **B9** gives promising anticancer activity with IC<sub>50</sub> of 6.65 μM, 18.44 μM and 24.71 μM, compared to that determined for PB and the other synthesized derivatives against the A549, MDA-MB and SW1116 lines, respectively. Compounds **B10** and **B15**, are also exhibited good anti-tumor activity against A549, MDA-MB and SW1116 cell lines with IC<sub>50</sub> of 17.30 μM, 17.61 μM and 18.07 μM, and with IC<sub>50</sub> of 6.84 μM, 23.74 μM and 17.65 μM, respectively. Overall, PB derivatives exhibited great potencies in inhibiting MDA-MB-231 than A549 and SW1116 cell lines.

MCF-10A, non-tumorigenic epithelial breast cell line, was used to investigate the toxicity of compounds against normal cell line and to determine the selectivity between cancer and the normal cell line.



Scheme 1. Synthesis of novel PB derivatives based on Passerini multicomponent reaction.

Results showed good selectivity of the compounds between the tumorigenic and non-tumorigenic cell lines. All the synthesized compounds, especially **B6**, **B9**, and **B10** showed greater specificity for human breast cancer cell with less damage to normal epithelial breast cell.

The structure-activity relationship study of the synthesized PB derivatives indicates that the basic structure (**B6** compound) showed the satisfactory effect in of A594, and MDA-MB-123 cell line growth repression rather than SW1116 cell line. The results synthesized compounds was changed by variation of substitution pattern in A-ring with CH<sub>3</sub>, OCH<sub>3</sub>, Cl, Br, F and NO<sub>2</sub> groups and substitution of C-ring with *t*-Bu rather than cyclohexyl. The existing one OCH<sub>3</sub> group on the A ring in the investigated basic structure gives an effective anti-tumor activity (with IC<sub>50</sub> less than 30 μM on all of the studied cell lines). Compounds **B3**, **B7**, **B12**, and **B13** substituted with methyl and halo groups in the *para* position of ring A showed negligible anti-tumor activity in the order of Cl > Me > F. On the other hand, **B12** which containing bromo group showed better antiproliferative activity against A549 and MDA-MB than other halo groups. However, by replacing the cyclohexyl ring with the *t*-Bu group in **B15**, the anticancer activity improved considerably compared to the **B3**.

Furthermore, the moving of the chloro group from *para* position to *meta* and *ortho* in ring A, increases the inhibitory activity on the three studied cancer cell lines. **B1** and **B2** which were substituted with an electron withdrawing nitro group showed moderate anti-cancer activity in the studied cancer cell lines. In comparison to the **B2** compound, replacement of the cyclohexyl ring with *t*-Bu in **B14** didn't show remarkable anticancer activity.

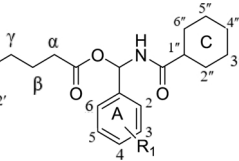
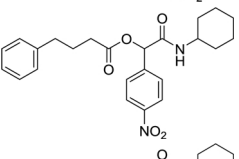
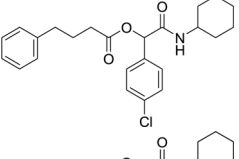
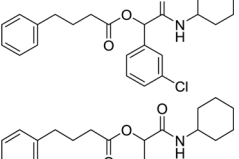
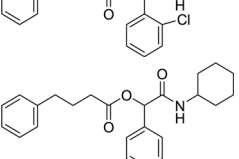
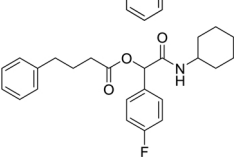
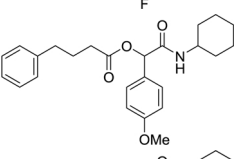
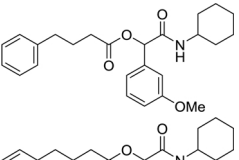
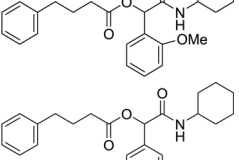
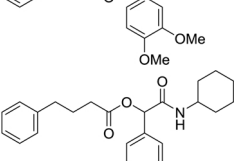
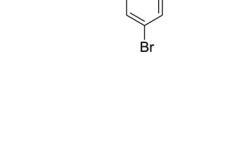

#### 2.2.1. Determining the apoptotic effect of B9 on MDA-MB-231 cell line

Apoptosis is a process of programmed cell death, which occurs to remove unnecessary and undesirable cells in multicellular organisms and plays a crucial role in tissue homeostasis. In the present study, the apoptotic effect of **B9** as one of the most effective compounds was evaluated by Annexin V/7AAD kit on the MDA-MB-231 cell line. In the early stages of apoptosis, the asymmetry of the plasma membrane is lost, and phosphatidylserin (PS), which is usually found on the inner layer of the plasma membranes, moves to the outer leaflet. A fluorochrome-labeled Annexin V specifically recognizes PS and binds to it. Also, a DNA binding 7-AAD reagent was used to identify healthy living cells by penetration into the nucleus of damaged cells such as late apoptotic or necrotic cells. To determine the apoptotic effect of **B9**, the MDA-MB-231 cell line was treated with three different concentrations (12, 18 and 36 μM) of this compound. Fig. 1 shows that, the percentages of apoptotic cells (Annexin V + cells) significantly increased from 5.44% at 12 μM to 90.9% at 36 μM with the increase in concentration. Accordingly, the number of live cells (Annexin V/7-AAD cells) remarkably decreased (93.0% to 6.16%). Results suggested that **B9** could induce apoptosis in cancerous cells (MDA-MB-231 cell line) in a dose-dependent manner.

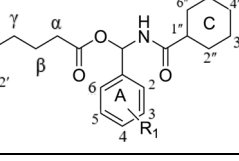
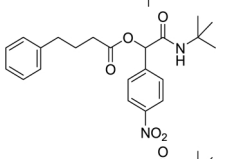
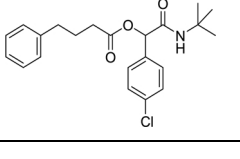
### 2.3. Molecular docking studies

As it was mentioned, histone deacetylases (HDAC) and pyruvate

**Table 1**  
The structure of the synthesized phenylbutyrate derivatives.

Name	Structure	Chemical Formula	%Yield	Reaction time (min/h)
B1		C <sub>24</sub> H <sub>28</sub> N <sub>2</sub> O <sub>5</sub>	97	15(min)
B2		C <sub>24</sub> H <sub>28</sub> N <sub>2</sub> O <sub>5</sub>	98	45(min)
B3		C <sub>24</sub> H <sub>28</sub> ClNO <sub>3</sub>	95	24(h)
B4		C <sub>24</sub> H <sub>28</sub> ClNO	96	50(min)
B5		C <sub>24</sub> H <sub>28</sub> ClNO	97	30(h)
B6		C <sub>24</sub> H <sub>29</sub> NO <sub>3</sub>	90	135(min)
B7		C <sub>24</sub> H <sub>28</sub> FNO <sub>3</sub>	94	180(min)
B8		C <sub>25</sub> H <sub>31</sub> NO <sub>4</sub>	89	33(h)
B9		C <sub>25</sub> H <sub>31</sub> NO <sub>4</sub>	91	26(h)
B10		C <sub>25</sub> H <sub>31</sub> NO <sub>4</sub>	84	22(h)
B11		C <sub>26</sub> H <sub>33</sub> NO <sub>5</sub>	90	24(h)
B12		C <sub>24</sub> H <sub>28</sub> BrNO <sub>3</sub>	93	65(min)

**Table 1 (continued)**

Name	Structure	Chemical Formula	%Yield	Reaction time (min/h)
B13		C <sub>25</sub> H <sub>31</sub> NO <sub>3</sub>	60	180(min)
B14		C <sub>22</sub> H <sub>26</sub> N <sub>2</sub> O <sub>5</sub>	80	40(min)
B15		C <sub>22</sub> H <sub>26</sub> ClNO <sub>3</sub>	82	28(h)

**Table 2**

*In vitro* cytotoxic activity of the synthesized compounds against three cancer cell lines: A549, MDA-MB-123 and SW1116 as well as normal breast line (MCF-10A).

Name	IC <sub>50</sub> (μM ± SD)			
	A594	MDA-MB-123	SW1116	MCF-10A
B1	64.44 ± 18.51	41.87 ± 1.75	64.56 ± 0.68	> 500
B2	76.80 ± 1.15	68.27 ± 3.72	76.63 ± 8.82	> 500
B3	440.36 ± 1.21	173.10 ± 0.33	> 500	> 500
B4	398.50 ± 1.60	68.26 ± 1.99	82.27 ± 1.26	> 500
B5	16.28 ± 0.62	36.141 ± 3.76	17.50 ± 1.28	> 500
B6	15.99 ± 0.27	18.65 ± 1.67	106.49 ± 0.96	> 500
B7	> 500	197.82 ± 12.11	> 500	> 500
B8	25.25 ± 3.69	25.83 ± 1.43	29.54 ± 0.44	> 500
B9	6.65 ± 0.07	18.44 ± 0.06	24.71 ± 0.52	> 500
B10	17.30 ± 0.26	17.61 ± 1.96	18.07 ± 0.54	> 500
B11	183.12 ± 0.08	32.11 ± 0.95	112.08 ± 2.13	> 500
B12	23.15 ± 2.69	32.11 ± 0.95	163.01 ± 3.90	> 500
B13	301.65 ± 4.93	143 ± 0.059	130.68 ± 1.07	> 500
B14	72.24 ± 0.77	40.80 ± 2.61	79.92 ± 8.08	> 500
B15	6.27 ± 0.63	23.74 ± 1.02	17.65 ± 0.95	> 500
PB	> 200	> 200	> 200	> 500

dehydrogenase kinase2 (PDK2) are the main target of PB as an anticancer agent. Here, molecular docking was conducted on the synthesized compounds, to elucidate their interactions and to obtain additional information in their molecular binding mode with PDK2 and HDAC targets. The results including the estimated free binding energy values ( $\Delta G_{\text{bind}}$ : expressed in kcalmol<sup>-1</sup>) for the best pose of the docked compounds, as well as the appropriate interactions with the main amino acid residues at the active site of the enzymes are shown in Figs. 2 and 3.

The range of the  $\Delta G_{\text{bind}}$  values were observed within -5.15 to -7.01 kcal mol<sup>-1</sup> for 2BU8 and -7.60 to -11.37 kcal mol<sup>-1</sup> for 1C3R. PB docking binding energy was -5.10 kcal mol<sup>-1</sup> and -4.11 kcal mol<sup>-1</sup> against 2BU8 and 1C3R, respectively. As shown in Table 3, most of the synthesized compounds showed better binding energy in compared to PB.

The docking binding energies of all the synthesized compounds on

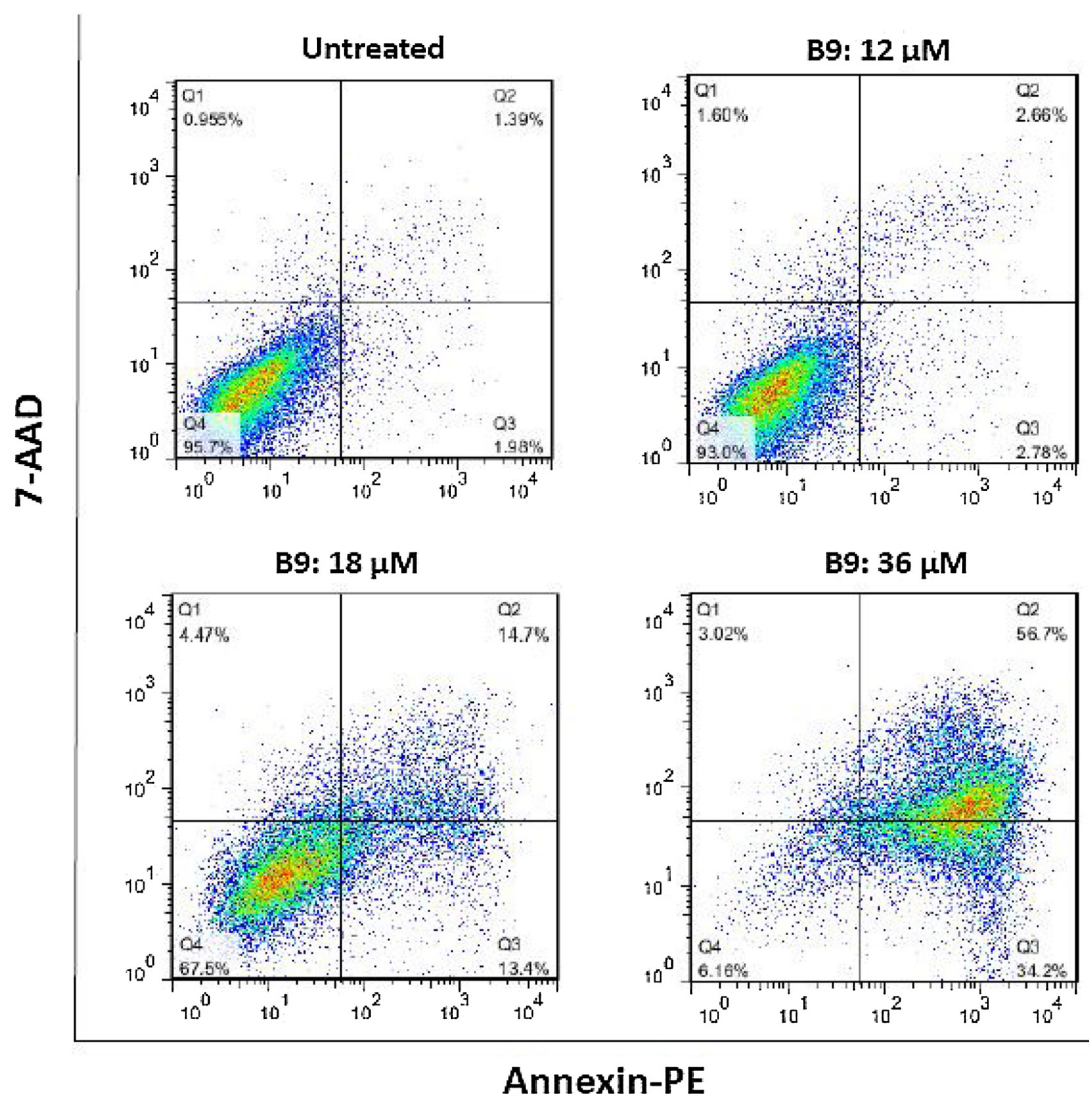


**Fig. 1.** Flow cytometry-based detection of the apoptotic properties of **B9** on the MDA-MB-231 cell line. Representative scatter plots show apoptosis of MDA-MB-231 cells after 72 h of incubation with different concentrations of **B9** (12, 18, and 36 μM) using the Annexin V-PE/7AAD detection kit. The percentages of apoptotic cells (Q2: late apoptotic and Q3: early apoptotic) were determined in Annexin V + cells. Q1: necrotic cells, Q2: late apoptotic cells, Q3: early apoptotic cells, and Q4: living cells.

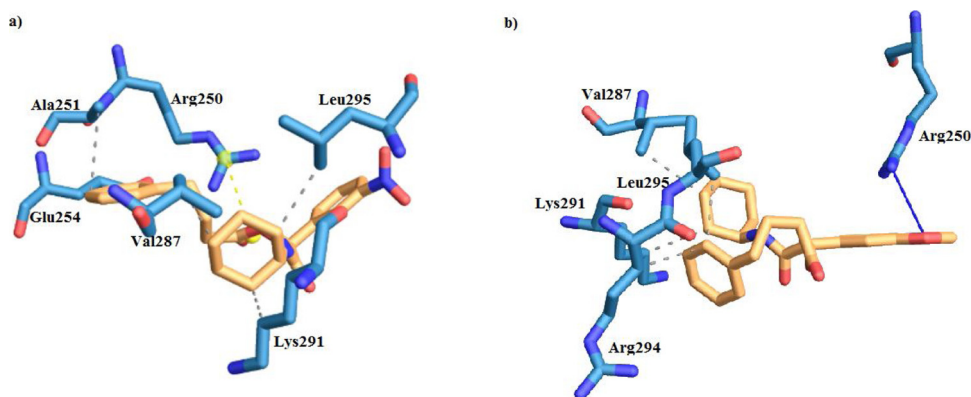


**Fig. 2.** Interactions of **B1** (a) and **B9** (b) with the residues in the binding site of PDK2 receptor.

both targets as well as their drug-likeness descriptors such as Molecular Weight (MW), logP, AlogP, H-Bond Acceptor (HBA), H-Bond Donor (HBD), Total Polar Surface Area (TPSA) and number of Rotatable Bond (nRB), for all of the synthesized compounds which were calculated

using DruLiTo, are shown in Table 3. All of the synthesized compounds pass the drug-likeness filter mainly Lipinski's rule of 5.

The interactions of the synthesized PB derivatives with PDK2 were investigated. As it was depicted in Fig. 2a, an electrostatic ionic bond

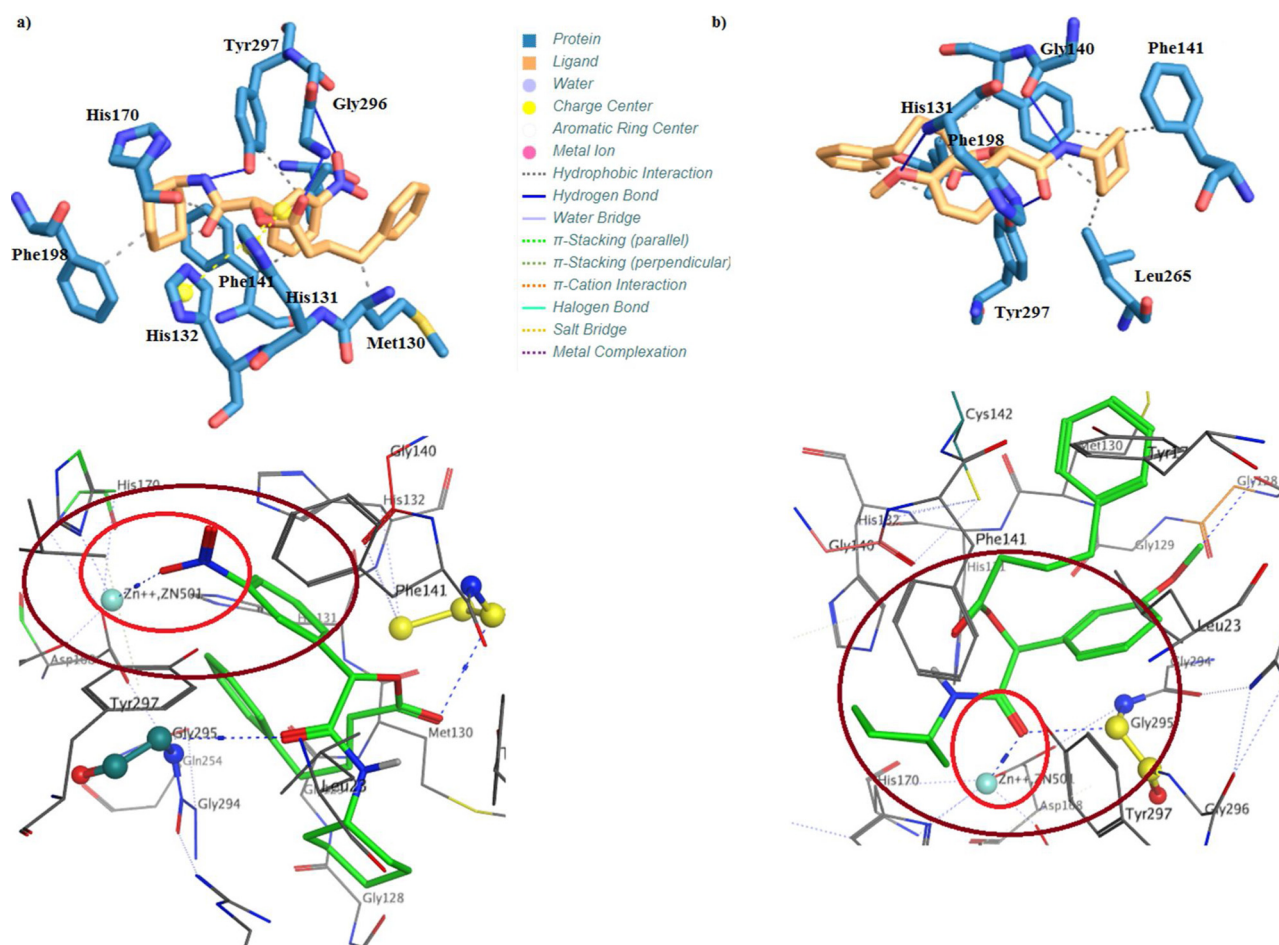


Fig. 3. Interactions of **B1** (a) and **B9** (b) with the residues in the binding site of HDAC receptor (1C3R).

Table 3

Molecular descriptor analysis and docking binding energy (Kcal/mol) on PDK2 and HDAC.

Name	$\Delta E(\text{Kcal/mol})^1$		MW <sup>2</sup>	XlogP	nDHB <sup>3</sup>	nAHB <sup>4</sup>	nRB <sup>5</sup>	tPSA <sup>6</sup>
	1C3R	2BU8						
<b>B1</b>	−9.56	−6.64	424.2	2.40	1	5	11	60.33
<b>B2</b>	−9.36	−6.42	424.2	2.40	1	5	11	60.33
<b>B3</b>	−9.49	−6.43	413.8	4.42	1	5	10	55.4
<b>B4</b>	−9.84	−7.01	413.8	4.42	1	5	10	55.4
<b>B5</b>	−8.62	−6.23	413.8	4.64	1	5	10	55.4
<b>B6</b>	−11.37	−6.34	379.21	4.48	1	5	10	55.4
<b>B7</b>	−9.67	−6.07	397.21	3.96	1	5	10	55.4
<b>B8</b>	−8.92	−6.27	409.23	4.09	1	5	11	64.63
<b>B9</b>	−9.79	−6.45	409.23	4.09	1	5	11	64.63
<b>B10</b>	−9.13	−6.09	409.23	4.30	1	5	11	64.63
<b>B11</b>	−7.60	−5.99	439.24	4.33	1	6	12	73.86
<b>B12</b>	−10.2	−6.63	457.13	4.60	1	4	11	55.4
<b>B13</b>	−9.73	−6.67	393.23	4.87	1	4	10	55.4
<b>B14</b>	−8.32	−5.15	398.18	1.87	1	4	11	60.33
<b>B15</b>	−8.35	−5.52	387.15	3.90	1	4	10	55.4
<b>PB</b>	−4.11	−5.10	164.08	4.22	1	2	4	37.3

<sup>1</sup> Docking binding energy.

<sup>2</sup> Molecular weight.

<sup>3</sup> Number of donor hydrogen bond.

<sup>4</sup> Number of acceptor hydrogen bond.

<sup>5</sup> Number of rotatable bond.

<sup>6</sup> Total polar surface area.

interaction exists between the carboxylate group of **B1** with Arg250 in the binding to 2BU8 (PDK2) receptor. The main interactions of this compound were hydrophobic interactions with Ala251, Glu254, Val287, Lys291, and Leu295. The most important residues in the binding of **B9** to 2BU8 target was hydrophobic interactions with Val287, Lys291, Arg294, and Leu295. A hydrogen bond interaction was also observed between the oxygen of methoxy group of **B9** with Arg250 (Fig. 2b).

In HDAC binding mode, Compound **B1** interacts *via* three types of interactions including hydrogen bond, ionic and hydrophobic interactions. As it was depicted in Fig. 3a, a hydrogen bond acceptor interaction between oxygen group of the ester carbonyl with Gly296. There is also existed a hydrogen bond donor interaction between NH of amide group with Tyr297 and an ionic interaction between carboxylate and His132. There are some hydrophobic interactions with Leu23, Met130, Phe141, His170, Phe198, and Tyr297. The high affinity of **B1** to the zinc ion in the active site of histone deacetylases (HDACs) through its Nitro group was also observed (Fig. 3a).

Compound **B9** interacts *via* its carbonyl of amide group with Zn. There is also existed some hydrogen bond interactions between oxygen of methoxy group with His131, NH of amide group with Gly140, and carbonyl of amide group with Tyr297 (Fig. 3b). Some hydrophobic interactions with Leu23, Phe141, Phe198, and Leu265 are also shown in Fig. 3b.

To verify the accuracy of docking results, its validating step is very important. So far, several methods have been introduced for docking validation (Yadav et al., 2012, 2017). Redocking of the Trichostatin A as the cocrystal ligand of 1C3R, indicated that the X-ray crystallography conformer was extremely identical to the docked conformer. RMSD of

docking for Trichostatin A in comparison with its coordination in the crystal structure was 1.12 Å. Nevertheless, to further verify validation of docking procedure, the docking validation was evaluated using receiver operating characteristic (ROC) and Enrichment Factor ( $EF_{max}$ ) (Granchi et al., 2015). In the first step, a set of 91 PDK2 inhibitors, and 52 HDAC inhibitors, which has been experimentally tested for their enzymatic inhibitory on these biological targets, were selected from ChEMBL database as SMILES format (Gaulton et al., 2012; Wassermann and Bajorath, 2011; Willighagen et al., 2013). Using DOCKFACE, an *in-house* batch script application, the 1D format of them were then changed to 3D mol2 format. These ligands were then based on their experimental  $IC_{50}$  classified into two subsets of active ligands and inactive decoys. Afterward, this ligands and decoys were docked to their receptors using the docking procedure which was applied to our synthesized compounds. As shown in Fig. 5, ROC plots are subsequently being obtained by plotting (Sensitivity (Se)) versus (1-Specificity (Sp)) for all docking scores. The more  $ROC_{AUC}$  value is, the better it can be distinguished between active ligands and inactive decoys.

The Enrichment Factor was also applied for docking validation. Compared to ROC plot, the  $EF_{max}$  factor is highly dependent on the number of ligands and decoys in a data set. But, ROC does not depend on the number of active ligands and inactive decoys and more valuable in making decisions about the validity of the methods than  $EF_{max}$  analysis. The plots and results of ROC and  $EF_{max}$  were provided for PDK2 and HDAC receptors are depicted in Fig. 4. The AUC of 0.772 and 0.868 on PDK2, and HDAC, respectively, showed that our applied docking procedure can clearly distinguished between active and inactive compounds.

### 3. Conclusion

To be concluded, a series of PB derivative using Passerini multi-component reaction was successfully synthesized and characterized. The cytotoxic activities of them against various human cancer cell lines including A549 (nonsmall cell lung cancer), MDA-MB-231 (breast cancer), and SW1116 (colon cancer) were evaluated. All the synthesized compounds showed remarkably higher antiproliferative activity than the parent anticancer agent, PB. Overall, they were more effective on the MDA-MB-231 cell line than the other studied cell lines. Results showed good selectivity of the compounds between the tumorigenic and non-tumorigenic epithelial breast cell line (MCF-10A). Among the

synthesized compounds, **B9** which exhibited high potency in inhibiting cell proliferation and significantly higher *in vitro* cytotoxic activity than the others, can effectively induce apoptosis in MDA-MB-231 cells in a dose-dependent manner. The Molecular docking studies of the synthesized compounds on pyruvate dehydrogenase kinase 2 (2BU8) and histone deacetylase complex (HDAC) confirmed that the investigated compounds could be used as potential candidates for new drug discovery in future.

### 4. General

All chemicals were obtained from Sigma Aldrich or Merck chemical companies. The Progress of the reactions was followed by TLC using silica gel polygrams SIL G/UV 254 plates or by GC using a Bruker gas chromatograph 450-GC, equipped with a flame ionization detector (FID) and a 3-meter length capillary column CP-SIL 5CB and nitrogen as the carrier gas. IR spectra were run on a Bruker's VERTEX 70 Series FT-IR Spectrometers. The  $^1H$  NMR and  $^{13}C$  NMR spectra were recorded on a Bruker Avance DPX 400 FT-NMR spectrometer ( $^1H$  NMR: TMS at 0.00 ppm,  $CDCl_3$  at 7.26 ppm, DMSO- $d_6$  at 2.50 ppm;  $^{13}C$  NMR:  $CDCl_3$  at 77.23 ppm, DMSO- $d_6$  at 39.51 ppm). All yields refer to the isolated products. Evaporation of solvents was performed at reduced pressure, with a Buchi rotary evaporator. The general melting point were recorded on an electrothermal digital melting point apparatus. Mass spectra was recorded on an Agilent Technologies 5975C GC-Mass spectrometer operating at an electron energy of 70 eV.

#### 4.1. Synthesis of phenylbutyrate analogs

A mixture of aldehyde derivatives (1 mmol, 1 equiv), isocyanide (1 mmol, 1 equiv) and phenylbutyrate was dissolved in 5 ml  $H_2O$ . The reaction mixture was stirred at room temperature for 15 min–48 h. The obtained white solid was filtered, washed with water and dried. If the residues were gross, they would be purified by recrystallization or plate chromatography (silica gel with 50% or 25% ethyl acetate in *n*-hexane). The physical and spectral data of selective are given below.

#### 4.2. 2-(cyclohexylamino)-1-(3-nitrophenyl)-2-oxoethyl 4-phenylbutyrate (B1)

Yield: 97.8%, mp: 105–108 °C, white solid. IR (KBr disk): (3312.19 (NH amid group)), (3086.53–3025.49 (CH aromatic)), (2933.98–2855.01 (CH aliphatic)), (1745.53 (C=O ester)), (1658.19 (C=O amid)), (1537.97 (NO<sub>2</sub> symmetric stretch)), (1537.97–1448.64 (C=C aromatic)), (1351.29 (NO<sub>2</sub> asymmetric stretch)), (1150.20 (C–O ester))  $cm^{-1}$ .  $^1H$  NMR (400 MHz, Chloroform- $d$ )  $\delta$  (8.25 (s, 1 H)  $H^2$ ), (8.20 (d,  $J$  = 8.2 Hz, 1 H)  $H^4$ ), (7.81 (d,  $J$  = 7.7 Hz, 1 H)  $H^6$ ), (7.55 (t,  $J$  = 7.9 Hz, 1 H)  $H^5$ ), (7.36 – 7.16 (m, 4 H)  $H^{2',3',5',6'}$  overlapping multiple), (7.14 (s, 1 H)  $H^4$ ), (6.18 – 6.10 (m, 1 H)  $CH^*$ ), 3.77 (dq,  $J$  = 14.5, 6.8, 5.1 Hz, 1 H)  $H^1$ ), (2.67 (t,  $J$  = 7.5 Hz, 2 H)  $H^{(c)}$ ), (2.49 (s, 2 H)  $H^{(a)}$ ), (2.08 – 1.87 (m, 4 H)  $H^{(b),2^{(a)},6^{(a)}}$ ), (1.78 – 1.55 (m, 4 H)  $H^{2^{(e)},6^{(e)},4^{(e)}}$ ), (1.17 (q,  $J$  = 11.5 Hz, 4 H)  $H^{3^{(e)},5^{(e)}}$ ).  $^{13}C$  NMR (100 MHz, Chloroform- $d$ )  $\delta$  172.25, 167.16, 141.72, 139.03, 134.75, 130.64, 129.50, 129.42, 127.21, 124.71, 122.73, 75.10, 49.43, 35.82, 34.29, 33.88, 27.15, 26.37, 25.70.

#### 4.3. 2-(cyclohexylamino)-1-(4-nitrophenyl)-2-oxoethyl 4-phenylbutanoate (B2)

Yield: 98%, mp: 102–104 °C, white solid. IR (KBr disk): (3270.76 (NH amid group)), (3087.13–3027.66 (CH aromatic)), (2932.33–2802.24 (CH aliphatic)), (1738.12 (C=O ester)), (1651.82 (C=O amid)), (1604.53–1416.29 (C=C aromatic)), (1523.10 (NO<sub>2</sub> symmetric stretch)), (1345.85 (NO<sub>2</sub> asymmetric stretch)), (1164.70 (C–O)  $cm^{-1}$ .  $^1H$  NMR (400 MHz, Chloroform- $d$ )  $\delta$  (8.21 (d,  $J$  = 8.5 Hz, 2 H)  $H^{3,5}$ ), (7.60 (d,  $J$  = 8.4 Hz, 2 H)  $H^{2,6}$ ), (7.41 – 7.16 (m, 4 H)  $H^{2',3',5',6'}$ ), (7.14

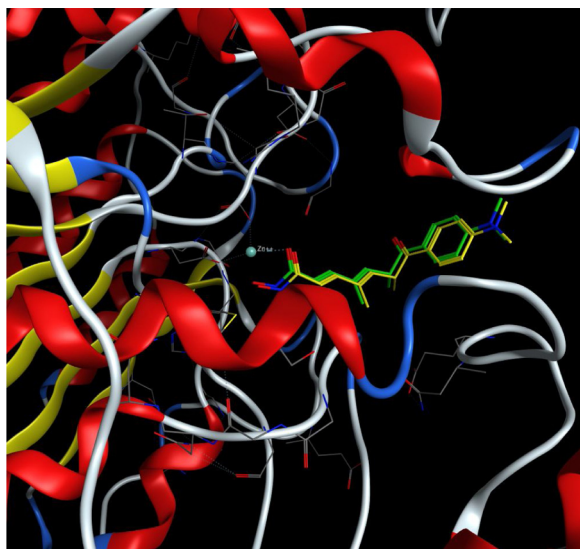
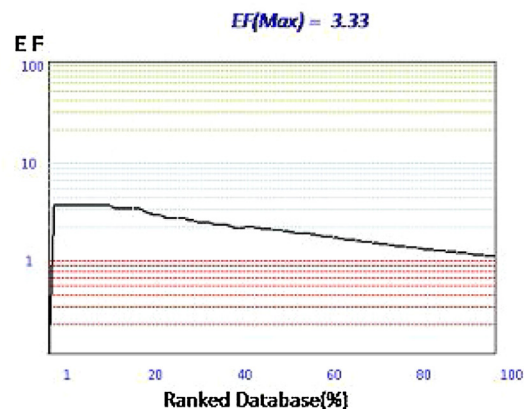
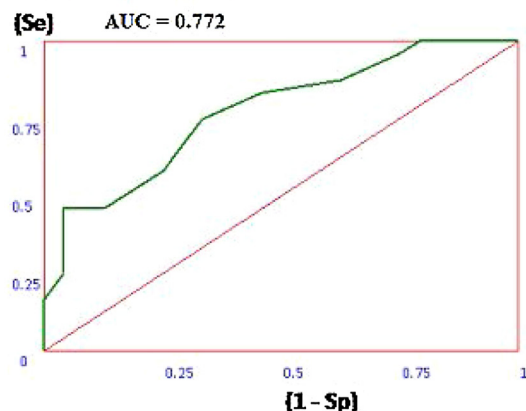


Fig. 4. Re-docking of the Trichostatin A as the co-crystal ligand of 1C3R, indicated that the X-ray crystallography conformer (the green model) was extremely identical to the docked conformer (the yellow model).

## a) Docking validation on PDK2 (2BU8)



## b) Docking validation on HDAC (1C3R)

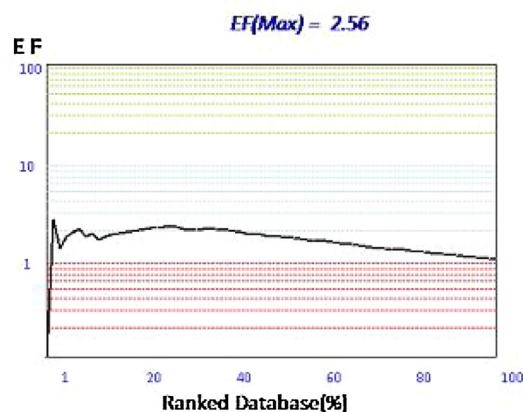
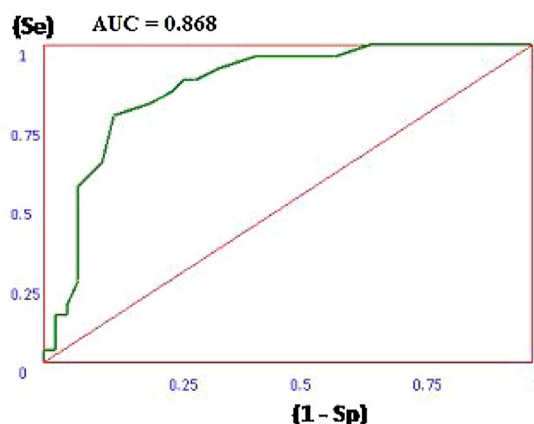


Fig. 5. ROC and EF diagrams a) for PDK2 (2BU8) receptor, b) for HDAC (1C3R) receptor.

(s, 1 H)  $H^{4'}$ ), (6.10 (s, 1 H)  $CH^*$ ), (3.76 (dtd,  $J = 14.0, 9.6, 9.1, 3.8$  Hz, 1 H)  $H^{1'}$ ), (2.69 (d,  $J = 7.6$  Hz, 2 H)  $H^{(v)}$ ), (2.49 (dt,  $J = 9.1, 4.6$  Hz, 2 H)  $H^{(a)}$ ), (2.06 – 1.86 (m, 4 H)  $H^{(B),2'(a),6'(e),4''}$ ), (1.34 (dq,  $J = 25.9, 13.9, 13.1$  Hz, 4 H)  $H^{2''(e),6''(e),4''}$ ), (1.25 – 0.92 (m, 4 H)  $H^{3'',5''}$ ).  $^{13}C$  NMR (100 MHz, Chloroform- $d$ )  $\delta$  172.25, 167.16, 141.72, 139.03, 134.75, 130.64, 129.50, 129.42, 127.21, 124.71, 122.73, 75.10, 49.43, 35.82, 34.29, 33.88, 27.15, 26.37, 25.70.

## 4.4. 1-(4-chlorophenyl)-2-(cyclohexylamino)-2-oxoethyl 4-phenylbutanoate (B3)

Yield: 96%, mp: 82–85 °C, white solid. IR (KBr disk): (3274.03 (NH amid group)), (3086.79–3029.30 (CH aromatic)), (2929.58–2854.23 (CH aliphatic)), (1745.39 (C=O ester)), (1647.47 (C=O amid)), (1563.58–1410.95 (C=C aromatic)), (1159.28 (C–O)), (754.90 (C–Cl))  $cm^{-1}$ .  $^1H$  NMR (400 MHz, Chloroform- $d$ )  $\delta$  (7.42 (dd,  $J = 5.7, 2.6$  Hz, 2 H)  $H^{2,6}$ ), (7.35 (dd,  $J = 5.2, 2.3$  Hz, 2 H)  $H^{3,5}$ ), (7.31 – 7.16 (m, 5 H)  $H^{2',3',4',5',6'}$ ), (6.06 (s, 1 H) CH), (3.77 (s, 1 H)  $H^{1'}$ ), (2.67 (d,  $J = 7.5$  Hz, 2 H)  $H^{(v)}$ ), (2.44 (dt,  $J = 6.9, 3.4$  Hz, 2 H)  $H^{(a)}$ ), (2.01 – 1.85 (m, 4 H)  $H^{(B),2'(a),6'(e)}$ ), (1.56 (s, 2 H)  $H^{2''(e),6''(e)}$ ), (1.38 (dd,  $J = 13.6, 10.2$  Hz, 2 H)  $H^{4''}$ ), (1.13 (p,  $J = 9.6, 9.0$  Hz, 4 H)  $H^{3'',5''}$ ).  $^{13}C$  NMR (100 MHz, Chloroform- $d$ )  $\delta$  173.06 – 171.19 (m), 167.80, 135.40 (d,  $J = 23.2$  Hz), 129.89, 129.74, 129.43, 127.12, 75.61, 49.22, 35.86, 34.39, 33.91, 27.23, 26.41, 25.68.

## 4.5. 1-(3-chlorophenyl)-2-(cyclohexylamino)-2-oxoethyl 4-phenylbutanoate (B4)

Yield: 96%, mp: 70–73 °C, white solid. IR (KBr disk): (3224.06 (NH

amid group)), (3080.35–3025.97 (CH aromatic)), (2933.07–2854.21 (CH aliphatic)), (1739.68 (C=O ester)), (1650.87 (C=O amid)), (1571.77–1413.39 (C=C aromatic)), (1164.44 (C–O)), (754.90 (C–Cl))  $cm^{-1}$ .  $^1H$  NMR (400 MHz, Chloroform- $d$ )  $\delta$  (7.41 (s, 1 H)  $H^{(v)}$ ), (7.31 (s, 2 H)  $H^{4,5}$ ), (7.31 – 7.18 (m, 4 H)  $H^{2',3',5',6'}$ ), (7.15 (d,  $J = 7.6$  Hz, 2 H)  $H^{6,4''}$ ), (6.03 (d,  $J = 6.4$  Hz, 1 H)  $CH^*$ ), (3.79 (dp,  $J = 15.2, 5.7, 4.9$  Hz, 1 H)  $H^{1'}$ ), (2.66 (t,  $J = 7.5$  Hz, 2 H)  $H^{(v)}$ ), (2.57 – 2.29 (m, 2 H)  $H^{(a)}$ ), (1.95 (dt,  $J = 24.4, 9.1$  Hz, 4 H)  $H^{(B),2'(a),6'(e)}$ ), (1.72 (s, 2 H)  $H^{2''(e),6''(e)}$ ), (1.51 – 1.31 (m, 2 H)  $H^{4''}$ ), (1.32 – 0.98 (m, 4 H)  $H^{3'',5''}$ ).  $^{13}C$  NMR (100 MHz, Chloroform- $d$ )  $\delta$  172.42, 167.73, 141.90, 138.77, 135.56, 130.95, 130.05, 129.46, 128.32, 127.13, 126.65, 75.55, 49.29, 35.84, 34.33, 33.88, 27.23, 26.40, 25.71.

## 4.6. 1-(2-chlorophenyl)-2-(cyclohexylamino)-2-oxoethyl 4-phenylbutanoate (B5)

Yield: 97%, mp: 74–76 °C, white solid. IR (KBr disk): (3308.64 (NH amid group)), (3061.78–3029.67 (CH aromatic)), (2938.15–2850.61 (CH aliphatic)), (1738.85 (C=O ester)), (1649.84 (C=O amid)), (1536.92–1449.65 (C=C aromatic)), (1133.88 (C–O)), (755.87 (C–Cl))  $cm^{-1}$ .  $^1H$  NMR (400 MHz, Chloroform- $d$ )  $\delta$  (7.53 (dd,  $J = 6.1, 3.3$  Hz, 1 H)  $H^{(v)}$ ), (7.46 – 7.22 (m, 5 H)  $H^{2',3',5',6',4'}$ ), (7.22 – 7.08 (m, 3 H)  $H^{4',5,6}$ ), (6.36 (s, 1 H)  $CH^*$ ), (3.80 (tdd,  $J = 10.5, 7.6, 4.2$  Hz, 1 H)  $H^{1'}$ ), (2.67 (t,  $J = 7.6$  Hz, 2 H)  $H^{(v)}$ ), (2.53 – 2.38 (m, 2 H)  $H^{(a)}$ ), (2.07 – 1.80 (m, 4 H)  $H^{(B),2'(a),6'(e)}$ ), (1.80 – 1.50 (m, 4 H)  $H^{2''(e),6''(e),4''}$ ), (1.38 – 1.13 (m, 4 H)  $H^{3'',4''}$ ).  $^{13}C$  NMR (100 MHz, Chloroform- $d$ )  $\delta$  173.01, 167.49, 142.12, 134.54, 131.13, 130.82, 130.62, 129.48, 129.40, 128.29, 127.03, 73.40, 49.35, 35.91, 34.31, 33.79, 33.70, 27.34, 26.43, 25.62.

## 4.7. 2-(cyclohexylamino)-2-oxo-1-phenylethyl 4-phenylbutanoate (B6)

Yield: 90%, mp: 75–78 °C, white solid. IR (KBr disk): (3273.02 (NH amid group)), (3087.77–3030.32 (CH aromatic)), (2925.82–2795.24 (CH aliphatic)), (1748.08 (C=O ester)), (1651.39 (C=O amid)), (1563.51–1412.90 (C=C aromatic)), (1152.30 (C–O))  $\text{cm}^{-1}$ .  $^1\text{H}$  NMR (400 MHz, Chloroform-d)  $\delta$  (7.44 – 7.13 (m, 10 H)  $\text{H}^{\text{Ring (A,B)}}$  overlapping multiple), (6.06 (s, 1 H)  $\text{CH}^*$ ), (3.77 (s, 1 H)  $\text{H}^{1'}$ ), (2.65 (t,  $J$  = 7.5 Hz, 2 H)  $\text{H}^{(v)}$ ), (2.44 (td,  $J$  = 7.2, 2.5 Hz, 2 H)  $\text{H}^{(\omega)}$ ), (1.96 (dq,  $J$  = 21.4, 7.5 Hz, 4 H)  $\text{H}^{(\beta),2'(\text{a}),6'(\text{a})}$ ), (1.56 (s, 2 H)  $\text{H}^{2'(\text{e}),6'(\text{e})}$ ), (1.43 – 1.25 (m, 2 H)  $\text{H}^{4'}$ ), (1.13 (p,  $J$  = 9.6, 9.0 Hz, 4 H)  $\text{H}^{3',4'}$ ).  $^{13}\text{C}$  NMR (100 MHz, Chloroform-d)  $\delta$  172.77, 168.36, 141.99, 136.88, 129.88, 129.70, 129.42, 128.41, 127.06, 76.35, 49.13, 35.88, 34.45, 33.90, 27.30, 26.43, 25.68.

## 4.8. 2-(cyclohexylamino)-1-(4-fluorophenyl)-2-oxoethyl 4-phenylbutanoate (B7)

Yield: 94%, mp: 85–87 °C, white solid. IR (KBr disk): (3275.31 (NH amid group)), (3090.73 (CH aromatic)), (2993.54–2855.35 (CH aliphatic)), (1745.63 (C=O ester)), (1648.92 (C=O amid)), (1566.20–1412.88 (C=C aromatic)), (1162.53 (C–O)), (C–F (978.85))  $\text{cm}^{-1}$ .  $^1\text{H}$  NMR (400 MHz, Chloroform-d)  $\delta$  [(7.40 (dd,  $J$  = 8.5, 5.3 Hz, 2 H)  $\text{H}^{2,6}$ ), (7.37 – 7.13 (m, 4 H)  $\text{H}^{2',3',5',6'}$ ), (7.04 (t,  $J$  = 8.5 Hz, 3 H)  $\text{H}^{3,5,4'}$  overlapping multiple], (6.02 (d,  $J$  = 6.4 Hz, 1 H)  $\text{CH}^*$ ), (3.79 (tdt,  $J$  = 11.5, 8.4, 4.0 Hz, 1 H)  $\text{H}^{1'}$ ), (2.65 (t,  $J$  = 7.5 Hz, 2 H)  $\text{H}^{(v)}$ ), (2.44 (td,  $J$  = 7.4, 2.8 Hz, 2 H)  $\text{H}^{(\omega)}$ ), (1.97 (dq,  $J$  = 18.9, 10.7, 9.1 Hz, 4 H)  $\text{H}^{(\beta),2'(\text{a}),6'(\text{a})}$ ), (1.67 – 1.51 (m, 2 H)  $\text{H}^{2'(\text{e}),6'(\text{e})}$ ), (1.49 – 1.30 (m, 2 H)  $\text{H}^{4'}$ ), (1.19 (dt,  $J$  = 20.0, 13.2 Hz, 4 H)  $\text{H}^{3',5'}$ ).  $^{13}\text{C}$  NMR (100 MHz, Chloroform-d)  $\delta$  172.51, 168.06, 165.93, 141.94, 130.43, 130.30, 129.43, 127.11, 116.85, 116.50, 75.62, 49.20, 35.86, 34.41, 33.95, 33.89, 27.26, 26.42, 25.70.

## 4.9. 2-(cyclohexylamino)-1-(4-methoxyphenyl)-2-oxoethyl 4-phenylbutanoate (B8)

Yield: 89%, mp: 90–93 °C, white solid. IR (KBr disk): (3279.53 (NH amid group)), (3077.52–3026.09 (CH aromatic)), (2934.89–2851.88 (CH aliphatic)), (1744.62 (C=O ester)), (1643.07 (C=O amid)), (1584.12–1411.67 (C=C aromatic)), (1150.67 (C–O))  $\text{cm}^{-1}$ .  $^1\text{H}$  NMR (400 MHz, Chloroform-d)  $\delta$  [(7.40 – 7.30 (m, 2 H)  $\text{H}^{2,6}$ ), (7.30 – 7.14 (m, 4 H)  $\text{H}^{2',3',5',6'}$ ), (7.12 (s, 1 H)  $\text{H}^{4'}$ ) overlapping multiple], (6.97 – 6.81 (m, 2 H)  $\text{H}^{3,5}$ ), (6.02 (d,  $J$  = 2.6 Hz, 1 H) CH group), (3.79 (s, 4 H) Me group &  $\text{H}^{1'}$ ), (2.64 (t,  $J$  = 7.6 Hz, 2 H)  $\text{H}^{(v)}$ ), (2.42 (td,  $J$  = 7.4, 2.9 Hz, 2 H)  $\text{H}^{(\omega)}$ ), (1.95 (dq,  $J$  = 23.0, 12.3, 9.8 Hz, 4 H)  $\text{H}^{(\beta),2'(\text{a}),6'(\text{a})}$ ), (1.64 (s, 2 H)  $\text{H}^{2'(\text{e}),6'(\text{e})}$ ), (1.36 (q,  $J$  = 11.2, 10.1 Hz, 2 H)  $\text{H}^{4'}$ ), (1.18 (dt,  $J$  = 23.4, 14.1 Hz, 4 H)  $\text{H}^{3',5'}$ ).  $^{13}\text{C}$  NMR (101 MHz, Chloroform-d)  $\delta$  172.71, 168.48, 156.90, 142.08, 130.03, 129.45, 129.40, 127.04, 115.15, 76.03, 56.28, 49.12, 35.89, 34.49, 33.98, 33.91, 27.32, 26.44, 25.70.

## 4.10. 2-(cyclohexylamino)-1-(3-methoxyphenyl)-2-oxoethyl 4-phenylbutanoate (B9)

Yield: 91%, mp: 86–89 °C, white solid. IR (KBr disk): (3251.24 (NH amid group)), (3090.37–3000.36 (CH aromatic)), (2927.45–2836.57 (CH aliphatic)), (1730.57 (C=O ester)), (1657.02 (C=O amid)), (1601.90–1463.15 (C=C aromatic)), (1137.34 (C–O))  $\text{cm}^{-1}$ .  $^1\text{H}$  NMR (400 MHz, Chloroform-d)  $\delta$  (7.44 – 7.18 (m, 5 H)  $\text{H}^{2',3',5',6',5}$ ), (7.16 (s, 1 H)  $\text{H}^{4'}$ ), (7.04 – 6.82 (m, 3 H)  $\text{H}^{2,4,6}$ ), (6.02 (d,  $J$  = 2.5 Hz, 1 H) CH group), (3.80 (s, 4 H)  $\text{H}^{(\text{OMe [m]})}$  &  $\text{H}^{1'}$ ), (2.65 (t,  $J$  = 7.7 Hz, 2 H)  $\text{H}^{(v)}$ ), (2.44 (t,  $J$  = 7.1 Hz, 2 H)  $\text{H}^{(\omega)}$ ), (2.01 (q,  $J$  = 7.5 Hz, 2 H)  $\text{H}^{(\beta)}$ ), (1.71 – 1.54 (m, 4 H)  $\text{H}^{2',6'}$ ), (1.39 – 1.25 (m, 2 H)  $\text{H}^{4'}$ ), (1.15 (q,  $J$  = 10.6 Hz, 4 H)  $\text{H}^{3',5'}$ ).  $^{13}\text{C}$  NMR (100 MHz, Chloroform-d)  $\delta$  172.58, 169.49 – 165.91 (m), 142.17, 139.12 – 136.06 (m), 130.77, 129.44, 127.07, 120.58, 115.53, 113.95, 76.20, 56.26, 49.15, 35.88, 34.43, 33.90,

27.30, 26.42, 25.69.

## 4.11. 2-(cyclohexylamino)-1-(2-methoxyphenyl)-2-oxoethyl 4-phenylbutanoate (B10)

Yield: 84%, mp: 92–95 °C, white solid. IR (KBr disk): (3252.47 (NH amid group)), (3080.85–3029.84 (CH aromatic)), (2929.16–2851.53 (CH aliphatic)), (1744.23 (C=O ester)), (1656.08 (C=O amid)), (1603.72–1463.43 (C=C aromatic)), (1261.32 (C–O))  $\text{cm}^{-1}$ .  $^1\text{H}$  NMR (400 MHz, Chloroform-d)  $\delta$  (7.47 (d,  $J$  = 7.6 Hz, 1 H)  $\text{H}^6$ ), (7.39 – 7.11 (m, 6 H)  $\text{H}^{5,2',3',4',5',6'}$ ), (7.07 – 6.86 (m, 2 H)  $\text{H}^{3,4}$ ), (6.35 (s, 1 H)  $\text{CH}^*$ ), (3.88 (s, 3 H)  $\text{H}^{(\text{OMe})}$ ), (3.76 (d,  $J$  = 9.6 Hz, 1 H)  $\text{H}^{1'}$ ), (2.67 (t,  $J$  = 7.6 Hz, 2 H)  $\text{H}^{(v)}$ ), (2.47 (q,  $J$  = 6.9 Hz, 2 H)  $\text{H}^{(\omega)}$ ), (1.99 (dq,  $J$  = 15.3, 7.7 Hz, 4 H)  $\text{H}^{(\beta),2'(\text{a}),6'(\text{a})}$ ), (1.58 (d,  $J$  = 11.1 Hz, 2 H)  $\text{H}^{2'(\text{e}),6'(\text{e})}$ ), (1.34 (t,  $J$  = 12.5 Hz, 2 H)  $\text{H}^{4'}$ ), (1.14 (dt,  $J$  = 34.8, 10.5 Hz, 4 H)  $\text{H}^{3',5'}$ ).  $^{13}\text{C}$  NMR (100 MHz, Chloroform-d)  $\delta$  173.33, 168.55, 157.34, 142.35, 130.94, 129.58, 129.52, 129.36, 126.95, 125.30, 122.16, 111.90, 71.11, 56.62, 48.90, 35.96, 34.47, 33.92, 33.68, 27.46, 26.49, 25.57, 25.51.

## 4.12. 2-(cyclohexylamino)-1-(3,4-dimethoxyphenyl)-2-oxoethyl 4-phenylbutanoate (B11)

Yield: 90%, mp: 107–110 °C, white solid. IR (KBr disk): (3252.56 (NH amid group)), (3082.96–3000.23 (CH aromatic)), (2923.97–2839.46 (CH aliphatic)), (1727.30 (C=O ester)), (1650.36 (C=O amid)), (1592.51–1425.76 (C=C aromatic)), (1144.24 (C–O))  $\text{cm}^{-1}$ .  $^1\text{H}$  NMR (400 MHz, Chloroform-d)  $\delta$  (7.34 – 7.08 (m, 5 H)  $\text{H}^{2',3',4',5',6'}$ ), (6.95 (d,  $J$  = 8.0 Hz, 2 H)  $\text{H}^{2,6}$ ), (6.83 (d,  $J$  = 8.2 Hz, 1 H)  $\text{H}^5$ ), (6.00 (s, 1 H)  $\text{CH}^*$ ), (3.86 (s, 7 H)  $\text{H}^{(\text{OMe [mP]})}$  &  $\text{H}^{1'}$ ), (2.65 (t,  $J$  = 7.6 Hz, 2 H)  $\text{H}^{(v)}$ ), (2.42 (d,  $J$  = 7.9 Hz, 2 H)  $\text{H}^{(\omega)}$ ), (1.95 (dq,  $J$  = 26.7, 10.9, 9.2 Hz, 4 H)  $\text{H}^{(\beta),2'(\text{a}),6'(\text{a})}$ ), (1.61 (d,  $J$  = 15.4 Hz, 2 H)  $\text{H}^{2'(\text{e}),6'(\text{e})}$ ), (1.35 (d,  $J$  = 12.4 Hz, 2 H)  $\text{H}^{4'}$ ), 1.11 (dd,  $J$  = 17.1, 7.2 Hz, 4 H)  $\text{H}^{3',5'}$ ).  $^{13}\text{C}$  NMR (100 MHz, Chloroform-d)  $\delta$  172.78, 168.41, 150.35 (d,  $J$  = 30.4 Hz), 142.07, 129.44, 127.07, 121.23, 112.06, 111.75, 76.18, 56.90, 49.16, 35.90, 34.48, 33.98, 33.88, 27.34, 26.43, 25.71.

## 4.13. 1-(4-bromophenyl)-2-(cyclohexylamino)-2-oxoethyl 4-phenylbutanoate (B12)

Yield: 94%, mp: 133–136 °C, white solid. IR (KBr disk): (3277.65 (NH amid group)), (3084.32–3029.23 (CH aromatic)), (2929.40–2854.45 (CH aliphatic)), (1744.66 (C=O ester)), (1648.05 (C=O amid)), (1560.52–1454.71 (C=C aromatic)), (1155.52 (C–O)), (C–Br (669.69))  $\text{cm}^{-1}$ .  $^1\text{H}$  NMR (400 MHz, Chloroform-d)  $\delta$  (7.49 (d,  $J$  = 8.2 Hz, 2 H)  $\text{H}^{3,5}$ ), (7.26 (d,  $J$  = 2.4 Hz, 5 H)  $\text{H}^{2',3',4',5',6'}$  overlapping multiple), (7.18 (d,  $J$  = 10.9 Hz, 2 H)  $\text{H}^{2,6}$ ), (5.99 (s, 1 H)  $\text{CH}^*$ ), (3.77 (d,  $J$  = 10.4 Hz, 1 H)  $\text{H}^{1'}$ ), (2.65 (t,  $J$  = 7.6 Hz, 2 H)  $\text{H}^{(v)}$ ), (2.45 (dt,  $J$  = 9.4, 4.8 Hz, 2 H)  $\text{H}^{(\omega)}$ ), 1.98 (tt,  $J$  = 22.2, 10.8 Hz, 4 H)  $\text{H}^{(\beta),2'(\text{a}),6'(\text{a})}$ ), [(1.65 (s, 2 H)  $\text{H}^{2'(\text{e}),6'(\text{e})}$ ), (1.36 (d,  $J$  = 12.5 Hz, 2 H)  $\text{H}^{4'}$ ), (1.22 (d,  $J$  = 34.0 Hz, 4 H)  $\text{H}^{3',5'}$ )] overlapping multiple].  $^{13}\text{C}$  NMR (100 MHz, Chloroform-d)  $\delta$  172.46, 167.80, 141.91, 135.96, 132.85, 130.05, 129.45, 127.13, 124.05, 75.65, 49.25, 35.87, 34.38, 33.92, 33.87, 27.25, 26.42, 25.71.

## 4.14. 2-(cyclohexylamino)-2-oxo-1-(p-tolyl)ethyl 4-phenylbutanoate (B13)

Yield: 93%, mp: 109–111 °C, white solid. IR (KBr disk): (3275.40 (NH amid group)), (3085.59–3028.15 (CH aromatic)), (2923.83–2853.91 (CH aliphatic)), (1745.14 (C=O ester)), (1648.44 (C=O amid)), (1562.49–1411.73 (C=C aromatic)), (1159.24 (C–O))  $\text{cm}^{-1}$ .  $^1\text{H}$  NMR (400 MHz, Chloroform-d)  $\delta$  (7.32 (dp,  $J$  = 15.8, 8.9, 8.1 Hz, 7 H)  $\text{H}^{2,6,2',3',4',5',6'}$ ), (7.15 (d,  $J$  = 6.5 Hz, 2 H)  $\text{H}^{3,5}$ ), (6.02 (d,  $J$  = 9.6 Hz, 1 H)  $\text{CH}^*$ ), (3.81 (ddt,  $J$  = 15.0, 10.4, 5.4 Hz, 1 H)  $\text{H}^{1'}$ ), (2.65 (t,  $J$  = 7.3 Hz, 2 H)  $\text{H}^{(v)}$ ), (2.45 (dd,  $J$  = 7.7, 3.3 Hz, 2 H)  $\text{H}^{(\omega)}$ ), (2.34 (s, 3 H)

Me group), (1.96 (dq,  $J = 19.5, 6.6, 5.7$  Hz, 4 H)  $H^{(B),2''(a),6''(a)}$ ), (1.62 (d,  $J = 16.2$  Hz, 2 H)  $H^{2''(e),6''(e)}$ ), (1.47 – 1.31 (m, 2 H)  $H^{4''}$ ), (1.18 (p,  $J = 13.2, 10.8$  Hz, 4 H)  $H^{3'',5''}$ ).  $^{13}\text{C}$  NMR (100 MHz, Chloroform- $d$ )  $\delta$  172.73, 168.53, 142.10, 139.84, 133.89, 130.42, 130.02, 129.47, 129.41, 128.47, 127.06, 76.26, 49.17, 35.91, 34.48, 34.26, 33.93, 33.88, 27.34, 26.45, 25.72, 22.21.

#### 4.15. 2-(tert-butylamino)-1-(4-nitrophenyl)-2-oxoethyl 4-phenylbutanoate (B14)

Yield: 80%, mp: 85–88 °C, white solid. IR (KBr disk): (3280.04 (NH amid group)), (3083.63–3025.98 (CH aromatic)), (2978.52–2937.44 (CH aliphatic)), (1741.28 (C=O ester)), (1653.88 (C=O amid)), (1606.27–1453.09 (C=C aromatic)), (1521.58 ( $\text{NO}_2$  symmetric stretch)), (1344.67 ( $\text{NO}_2$  asymmetric stretch)), (1141.07 (C–O ester)  $\text{cm}^{-1}$ ).  $^1\text{H}$  NMR (400 MHz, Chloroform- $d$ )  $\delta$  (8.47 – 8.03 (m, 3 H)  $H^{(NH),3,5}$ ), (7.59 (d,  $J = 8.4$  Hz, 2 H)  $H^{2,6}$ ), (7.36 – 7.09 (m, 5 H)  $H^{2',3',4',5',6'}$ ), (6.02 (d,  $J = 5.1$  Hz, 1 H)  $\text{CH}^*$ ), (2.67 (t,  $J = 7.5$  Hz, 2 H)  $H^{(v)}$ ), (2.49 (dt,  $J = 9.5, 4.8$  Hz, 2 H)  $H^{(w)}$ ), (2.02 (q,  $J = 7.4$  Hz, 2 H)  $H^{(B)}$ ), (1.35 (s, 9 H)  $H^{[3 \text{ Me group}]}$ ).  $^{13}\text{C}$  NMR (100 MHz, Chloroform- $d$ )  $\delta$  172.22, 167.04, 149.04, 143.96, 141.72, 129.51, 129.41, 129.01, 127.24, 124.82, 75.44, 52.83, 35.83, 34.30, 29.61, 27.17.

#### 4.16. 2-(tert-butylamino)-1-(4-chlorophenyl)-2-oxoethyl 4-phenylbutanoate (B15)

Yield: 82%, mp: 104–107 °C, white solid. IR (KBr disk): (3305.92 (NH amid group)), (3083.99–3063.24 (CH aromatic)), (2975.71–2864.92 (CH aliphatic)), (1735.81 (C=O ester)), (1657.39 (C=O amid)), (1599.10–1410.09 (C=C aromatic)), (1232.93 (C–O ester), (700.47 (C–Cl))  $\text{cm}^{-1}$ ).  $^1\text{H}$  NMR (400 MHz, Chloroform- $d$ )  $\delta$  (7.55 – 7.09 (m, 9 H)  $H^{2,3,5,6,2',3',4',5',6'}$  overlapping multiple), (5.92 (s, 1 H)  $\text{CH}^*$ ), (2.65 (t,  $J = 7.6$  Hz, 2 H)  $H^{(v)}$ ), (2.43 (td,  $J = 7.3, 2.6$  Hz, 2 H)  $H^{(w)}$ ), (1.98 (p,  $J = 7.6$  Hz, 2 H)  $H^{(B)}$ ), (1.34 (s, 9 H)  $H^{[3 \text{ Me groups}]}$ ).  $^{13}\text{C}$  NMR (100 MHz, Chloroform- $d$ )  $\delta$  172.46, 167.90, 162.43, 141.89 (d,  $J = 21.5$  Hz), 135.80 (d,  $J = 14.8$  Hz), 129.91, 129.76, 129.44, 127.13, 75.77, 35.86, 34.41, 29.64, 27.25.

## 5. Biological assay

### 5.1. Cell lines and cell culture

Human lung adenocarcinoma epithelial cell line (A549, ATCC® CCL-185™), breast adenocarcinoma (MDA-MB-231, ATCC® HTB-26™), human oral epidermoid carcinoma cell line (KB, ATCC® CCL-17™) and human colon cancer cell line (SW116, ATCC® CCL-233™), were obtained from National Cell Bank of Iran (NCBI, Pasteur Institute, Tehran, Iran). All cell lines were cultured in DMEM culture supplemented with 10% fetal bovine serum (FBS) and 1% penicillin-streptomycin at 37 °C in the humidified  $\text{CO}_2$  incubator.

Cytotoxic activity of all the synthesized compounds was performed by standard 3-(4,5-dimethylthiazol-yl)-2,5-diphenyl-tetrazolium bromide (MTT) assay. The cells were harvested and plated in 96-well microplates at a density of  $1 \times 10^4$  cells per well in 100  $\mu\text{l}$  complete culture medium (containing fetal bovine serum and antibiotics). After 24 h incubation, each cell was treated with seven different concentrations of the compounds ranging from 5 to 500  $\mu\text{M}$  in triplicate. Different concentrations of PB were also used as positive controls. Three untreated wells were considered as negative controls. After 72 h, media were replaced with 100  $\mu\text{l}$  media containing 0.5 mg/ml of MTT solution. Then media containing MTT were discarded and 100  $\mu\text{l}$  dimethylsulfoxide (DMSO) was added to each well to dissolve the formazan crystals. The solutions were incubated overnight. The absorbance in individual wells was determined at 570 nm by a Bio-Rad microplate reader (Model 680). Data was calculated and expressed as the 50% inhibitory concentrations ( $\text{IC}_{50}$ ). Each experiment was independently repeated three times. Data

are presented as mean  $\pm$  SEM.

### 5.2. Apoptosis assay

BioLegend's PE Annexin V Apoptosis Detection Kit with 7AAD (Biolegend, USA) was used to assess the apoptotic effect of B9 as previously described (Fereidoonzhad et al., 2018a,b). Briefly,  $0.5 \times 10^5$  cells per 1 ml of complete culture medium were seeded in a 24-well culture plate, treated with B9 compound in different concentrations (12, 18, and 36  $\mu\text{M}$ ) for 72 h. An untreated sample was also included as a negative control. Treated and untreated cells were then harvested and washed twice with cold BioLegend's Cell Staining Buffer, transferred to the polystyrene round-bottom tubes (BD Bioscience, USA) and stained with 2  $\mu\text{l}$  of PE-conjugated Annexin V and 2  $\mu\text{l}$  of 7-AAD solution for 15 min at room temperature in the dark. 300  $\mu\text{l}$  of Binding Buffer was added to each tube and analyzed immediately by four-color FACSCalibur flow cytometer (BD Bioscience, USA) with proper setting. The data were analyzed by FlowJo software packages.

### 5.3. Molecular docking of synthesized compounds on PDK2 and HDAC

The three-dimensional crystal structures of PDK2 (PDB ID: 2BU8) and HDAC (PDB ID: 1C3R) enzymes were obtained from the protein data bank ([www.rcsb.org/pdb](http://www.rcsb.org/pdb)). Water molecules and co-crystal ligands (dichloroacetate and trichostatin-A for PDK2 and HDAC enzymes, respectively) were removed from the 3D crystal structures. Subsequently, the enzymes were converted to PDBQT and gasteiger partial charges were added using MGLTOOLS 1.5.6 (Morris et al., 2008). The initial structure of each synthesized PB derivatives was drawn and optimized by the ChemBioDraw (version 12.0) and Hyperchem (Version 8, Hypercube Inc., Gainesville, FL, USA) software, respectively. In the minimization procedure by using Hyperchem package, each compound was optimized with molecular mechanics (MM+) method and then quantum-based semiempirical method (AM1). After that, the output results of optimized structures were converted to PDBQT using MGLtools. Finally, docking was performed on flexible compounds and rigid receptors by an *in-house* batch script (DOCKFACE) of AutoDock 4.2 based on the Lamarckian genetic algorithm. The binding sites were defined as: all amino acid residues within grid box with dimensions (40, 50, and 50) Å from dichloroacetate present in the PDK2, all amino acid residues within grid box with dimensions (40, 40, and 40) Å from trichostatin-A present in the HDAC enzyme. The grid was set in 0.375-Å spacing. Binding interactions between docked potent agents and the targets were analyzed using Autodock tools program (ADT, Version 1.5.6) and PLIP (fully automated protein–ligand interaction profiler) (34) and the lowest docking binding energy conformation was chosen as the best binding mode concerning the AutoDock scoring function.

## Acknowledgments

The authors would like to thank research deputy Ahvaz Jundishapur University of medical sciences who support this work. Collaboration of Cancer, Environmental and Petroleum Pollutants Research Center and medicinal chemistry department, school of pharmacy, Ahvaz Jundishapur University of Medical Sciences, in providing the required facilities for this work is greatly acknowledged. This article was extracted from thesis by Raheleh Baghgoi (CRC-9710).

## References

- Burrage, L.C., Jain, M., Gandolfo, L., Lee, B.H., Nagamani, S.C., Consortium, U.C.D., 2014. Sodium phenylbutyrate decreases plasma branched-chain amino acids in patients with urea cycle disorders. *Mol. Genet. Metab.* 113 (1), 131–135.
- Doherty, J.R., Cleveland, J.L., 2013. Targeting lactate metabolism for cancer therapeutics. *J. Clin. Invest.* 123 (9), 3685–3692.
- Dömling, A., 2002. Recent advances in isocyanide-based multicomponent chemistry. *Curr. Opin. Chem. Biol.* 6 (3), 306–313.

- Donohoe, D.R., Collins, L.B., Wali, A., Bigler, R., Sun, W., Bultman, S.J., 2012. The Warburg effect dictates the mechanism of butyrate-mediated histone acetylation and cell proliferation. *Mol. Cell* 48 (4), 612–626.
- Fereidoonzehad, M., Shahsavari, H.R., Abedanzadeh, S., Behchenari, B., Hossein-Abadi, M., Faghih, Z., et al., 2018a. Cycloplatinated(II) complexes bearing 1,1'-bis(diphenylphosphino)ferrocene ligand: biological evaluation and molecular docking studies. *New J. Chem.* 42 (4), 2385–2392.
- Fereidoonzehad, M., Shahsavari, H.R., Lotfi, E., Babaghasabha, M., Fakhri, M., Faghih, Z., et al., 2018b. (benzyl isocyanide)gold(I) pyrimidine-2-thiolate complex: synthesis and biological activity. *Appl. Organomet. Chem.* 32 (3), e4200.
- Ferriero, R., Brunetti-Pierri, N., 2013. Phenylbutyrate increases activity of pyruvate dehydrogenase complex. *Oncotarget* 4 (6), 804.
- Ferriero, R., Manco, G., Lamantea, E., Nusco, E., Ferrante, M.I., Sordino, P., et al., 2013. Phenylbutyrate therapy for pyruvate dehydrogenase complex deficiency and lactic acidosis. *Sci. Transl. Med.* 5 (175) 175ra31-ra31.
- Ferriero, R., Boutron, A., Brivet, M., Kerr, D., Morava, E., Rodenburg, R.J., et al., 2014. Phenylbutyrate increases pyruvate dehydrogenase complex activity in cells harboring a variety of defects. *Ann. Clin. Transl. Neurol.* 1 (7), 462–470.
- Gardian, G., Yang, L., Cleren, C., Calingasan, N.Y., Klivenyi, P., Beal, M.F., 2004. Neuroprotective effects of phenylbutyrate against MPTP neurotoxicity. *Neuromol. Med.* 5 (3), 235–241.
- Gaulton, L., Bellis, L.J., Bento, A.P., Chambers, J., Davies, M., Hersey, A., et al., 2012. ChEMBL: a large-scale bioactivity database for drug discovery. *Nucleic Acids Res.* 40 (Database issue):D1100-7.
- Gore, S.D., Samid, D., Weng, L.-J., 1997. Impact of the putative differentiating agents sodium phenylbutyrate and sodium phenylacetate on proliferation, differentiation, and apoptosis of primary neoplastic myeloid cells. *Clin. Cancer Res.* 3 (10), 1755–1762.
- Granchi, C., Capecchi, A., Del Frate, G., Martinelli, A., Macchia, M., Minutolo, F., et al., 2015. Development and validation of a docking-based virtual screening platform for the identification of new lactate dehydrogenase inhibitors. *Molecules* 20 (5), 8772–8790.
- Iannitti, T., Palmieri, B., 2011. Clinical and experimental applications of sodium phenylbutyrate. *Drugs* 11 (3), 227–249.
- Jeng, J.-H., MY-P, Kuo, Lee, P.-H., Wang, Y.-J., Lee, M.-Y., Lee, J.-J., et al., 2006. Toxic and metabolic effect of sodium butyrate on SAS tongue cancer cells: role of cell cycle deregulation and redox changes. *Toxicology* 223 (3), 235–247.
- Jin, X., Wu, N., Dai, J., Li, Q., Xiao, X., 2017. TXNIP mediates the differential responses of A549 cells to sodium butyrate and sodium 4-phenylbutyrate treatment. *Cancer Med.* 6 (2), 424–438.
- Kusaczuk, M., Krętowski, R., Bartoszewicz, M., Cechowska-Pasko, M., 2016. Phenylbutyrate—a pan-HDAC inhibitor—suppresses proliferation of glioblastoma LN-229 cell line. *Tumor Biol.* 37 (1), 931–942.
- Li, L.-Z., Deng, H.-X., Lou, W.-Z., Sun, X.-Y., Song, M.-W., Tao, J., et al., 2012. Growth inhibitory effect of 4-phenyl butyric acid on human gastric cancer cells is associated with cell cycle arrest. *World J. Gastroenterol.* 18 (1), 79.
- Morris, G.M., Huey, R., Olson, A.J., 2008. Using AutoDock for ligand-receptor docking. *Current protocols in bioinformatics / editorial board. Andreas D Baxevanis [et al] Chapter 8:Unit 8 14.*
- Özcan, U., Yilmaz, E., Özcan, L., Furuhashi, M., Vaillancourt, E., Smith, R.O., et al., 2006. Chemical chaperones reduce ER stress and restore glucose homeostasis in a mouse model of type 2 diabetes. *Science* 313 (5790), 1137–1140.
- Rada-Iglesias, A., Enroth, S., Ameur, A., Koch, C.M., Clelland, G.K., Respuela-Alonso, P., et al., 2007. Butyrate mediates decrease of histone acetylation centered on transcription start sites and down-regulation of associated genes. *Genome Res.* 17 (6), 708–719.
- Rajendran, J.G., Mankoff, D.A., O'Sullivan, F., Peterson, L.M., Schwartz, D.L., Conrad, E.U., et al., 2004. Hypoxia and glucose metabolism in malignant tumors: evaluation by [18F] fluoromisonidazole and [18F] fluorodeoxyglucose positron emission tomography imaging. *Clin. Cancer Res.* 10 (7), 2245–2252.
- Ricobaraza, A., Cuadrado-Tejedor, M., Perez-Mediavilla, A., Frechilla, D., Del Rio, J., Garcia-Osta, A., 2009. Phenylbutyrate ameliorates cognitive deficit and reduces tau pathology in an Alzheimer's disease mouse model. *Neuropsychopharmacology* 34 (7), 1721–1732.
- Seyfried, T.N., Shelton, L.M., 2010. Cancer as a metabolic disease. *Nutr. Metab.* 7, 7.
- Singh, O.V., Vij, N., Mogayzel, P.J., Jozwik, C., Pollard, H.B., Zeitlin, P.L., 2006. Pharmacoproteomics of 4-phenylbutyrate-treated IB3-1 cystic fibrosis bronchial epithelial cells. *J. Proteome Res.* 5 (3), 562–571.
- Villar-Garea, A., Esteller, M., 2004. Histone deacetylase inhibitors: understanding a new wave of anticancer agents. *Int. J. Cancer* 112 (2), 171–178.
- Warburg, O., Wind, F., Negelein, E., 1927. The metabolism of tumors in the body. *J. Gen. Physiol.* 8 (6), 519.
- Wassermann, A.M., Bajorath, J., 2011. BindingDB and ChEMBL: online compound databases for drug discovery. *Expert Opin. Drug Discov.* 6 (7), 683–687.
- Willighagen, E.L., Waagmeester, A., Spjuth, O., Ansell, P., Williams, A.J., Tkachenko, V., et al., 2013. The ChEMBL database as linked open data. *J. Cheminform.* 5 (1), 23.
- Yadav, D.K., Khan, F., Negi, A.S., 2012. Pharmacophore modeling, molecular docking, QSAR, and in silico ADMET studies of gallic acid derivatives for immunomodulatory activity. *J. Mol. Model.* 18 (6), 2513–2525.
- Yadav, D.K., Kumar, S., Saloni, Singh H., Kim, M.H., Sharma, P., et al., 2017. Molecular docking, QSAR and ADMET studies of withanolide analogs against breast cancer. *Drug Des. Devel. Ther.* 11, 1859–1870.
- Zhang, W., Zhang, S.-L., Hu, X., Tam, K.Y., 2015. Targeting tumor metabolism for cancer treatment: is pyruvate dehydrogenase kinases (PDKs) a viable anticancer target? *Int. J. Biol. Sci.* 11 (12), 1390.
- Zhang, W., S.-L, Zhang, Hu, X., Tam, K.Y., 2017. Phenyl butyrate inhibits pyruvate dehydrogenase kinase 1 and contributes to its anti-cancer effect. *Eur. J. Pharm. Sci.* 110, 93–100.